Chapter 4
Optical and structural properties of CCSVT- grown $CuGaSe_2$ thin films

Film growth conditions governe defect chemistry and composition, which in turn affect the structural, optical and electrical properties of $CuGaSe_2$. In this chapter results of optical, structural and compositional characterizations of CCSVT- grown $CuGaSe_2$ thin films as a function of composition are presented. In section 4.1 the absorption coefficient of $CuGaSe_2$ films is determined for different compositions ([Ga]/[Cu]) from transmission, T, and reflection, R, measurements, while section 4.2 deals with the microstructural investigations. Elemental depth profiles of $CuGaSe_2$ films are presented in section 4.3

4.1 Absorption coefficient and optical band gap

The aim of this investigation is to investigate the influence of the film composition on the $CuGaSe_2$ fundamental absorption edge. The absorption coefficient of $CuGaSe_2$ thin films deposited on soda lime glass (SLG) with defined thickness and composition, i.e. determined [Ga]/[Cu] ratio, has been investigated by means of optical transmission and reflection at 300 K, assuming that all light intensity not transmitted is absorbed by the thin films and neglecting the effect of the SLG/thin film interface, using equation 4.1 [61]

$$\alpha = -\frac{1}{d}\ln\left(\frac{\sqrt{(1-R)^4 + 4T^2R^2} - (1-R)^2}{2TR^2}\right) \tag{4.1}$$

where α is the absorption coefficient, d is the thickness of the film, and T and R are the transmission and reflectance, respectively. The results obtained have been plotted in figure 4.1 as a function of energy of the incident photons for a [Ga]/[Cu] ratio ranging from 0.95 to 1.29 (table 3.1).

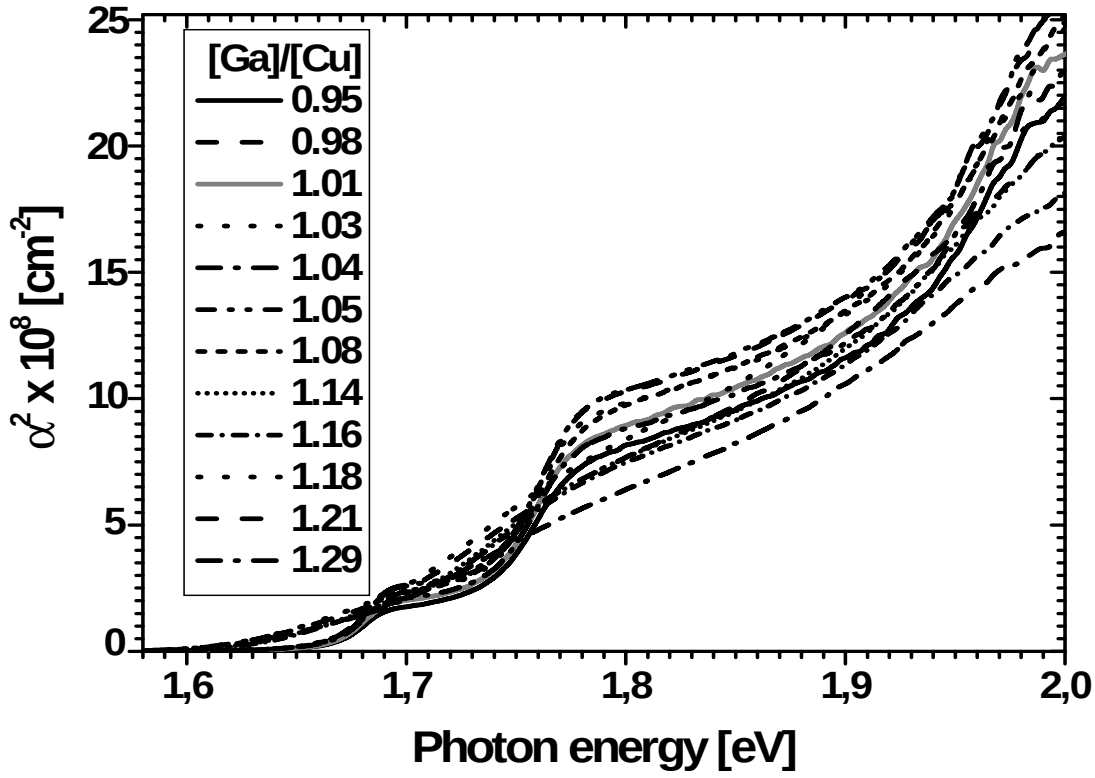

Figure 4.1. *Square of absorption coefficient in dependence of the photon energy measured on CCSVT- grown $CuGaSe_2$ thin films with different [Ga]/[Cu] ratios (table 3.1). From these plots, three fundamental optical absorptions at 1.67 eV, 1.75 eV and 1.93 eV are extracted with an uncertainty of about ± 0.05 eV.*

For $CuGaSe_2$ material, the valence- band maximum is composed of three nondegenerate states, giving rise to three transitions called $E_0(A)$, $E_0(B)$, and $E_0(C)$ from smaller to larger energy. In a simplified model, $E_0(A)$ and $E_0(B)$ are regarded as a crystal-field-split gap, and the higher energy $E_0(C)$ transition corresponds to the spin-orbit-split gap. Usually, these three transitions are resolved for the $CuGaSe_2$ films [63], which is also the case in the absorption spectra α for the CCSVT-grown $CuGaSe_2$ thin films. The $\alpha^2 = f(h\nu)$ curves of $CuGaSe_2$ were plotted since in the case of allowed direct interband transitions (in the simple parabolic two- band model) in the absence of electron- hole interactions, the absorption coefficient α has the following spectral dependence [62]:

$$\alpha\,(hv) \propto (h\nu - E_g)^{1/2} \text{ for } hv > E_g \tag{4.2}$$

where E_g is the corresponding semiconductor band gap. In this case, E_g is associated with the three energies $E_0(A)$, $E_0(B)$, and $E_0(C)$ of the $CuGaSe_2$ fundamental absorption. The analysis of the absorption coefficient spectra revealed the presence of three optical transitions at the photon energies of approximately 1.67 eV, 1.75 eV, and 1.93 eV. A "red shift" of the absorption edge with increasing [Ga]/[Cu] ratio is observed, as well as a broadening of the $CuGaSe_2$ distinct structure corresponding to the three band-to-band transitions described above. The observed broadening of the spectra in Ga-rich $CuGaSe_2$ can be explained both

by the effect of shrinking of the $CuGaSe_2$ crystalline unit cell with increasing Ga content [64] and by the high doping and compensation on the band structure of semiconductors. The latter effect is described by the model of fluctuating potentials [39]. Thus, the energies E_0(A), E_0(B), and E_0(C) can be determined as a function of the [Ga]/[Cu] ratio by extrapolation of the linear parts of the respective $(\alpha_{1,2,3})^2 = f(h\nu)$ curve (figure 4.1) to zero, where α_1, α_2, and α_3 are the absorption coefficient data extracted from the energy range of the corresponding transition from the general $\alpha = f(h\nu)$ spectra. The data obtained are presented in figure 4.2.

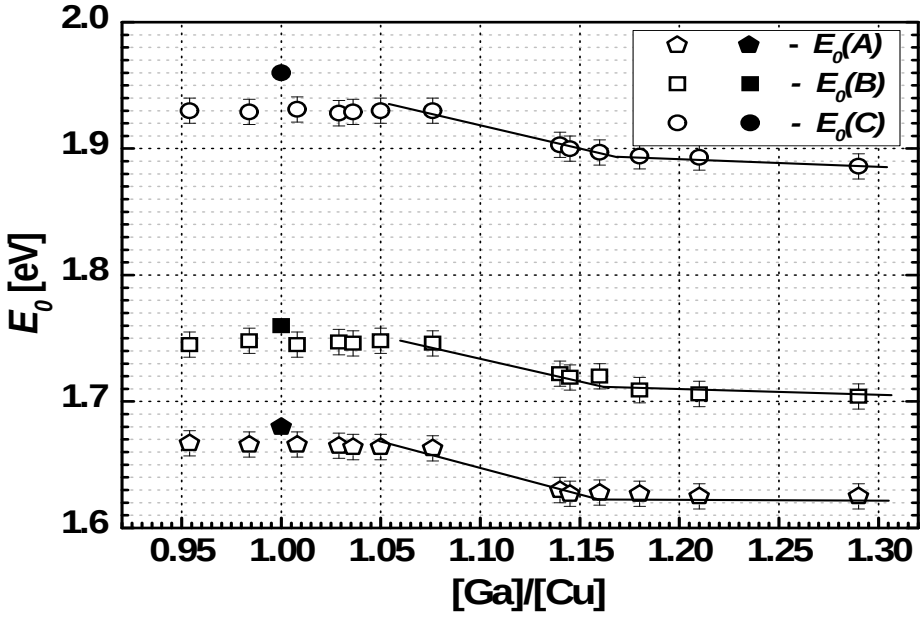

Figure 4.2. *The extracted energy transitions E_0(A), E_0(B), and E_0(C) at the fundamental absorption edge of $CuGaSe_2$ thin films with varying [Ga]/[Cu] ratio at room temperature. E_0(A) and E_0(B) transitions are related to the crystal-field-split gap, while the higher energy E_0(C) transition corresponds to the spin-orbit-split gap. The open symbols represent the data extracted from the $\alpha^2 = f(h\nu)$ curves in figure 4.1, and the full symbols display the reported values from the literature* [65]

It is worthwhile mentioning that the E_0(A), E_0(B), and E_0(C) values at [Ga]/[Cu] = 1.0 are close to those reported in Ref [65]. All the curves exhibit similar behavior and almost constant values are observed up to a composition corresponding to [Ga]/[Cu] = 1.05. These results are consistent with those obtained by Mikkelsen [21] stating that the homogeneity range of the chalcopyrite phase extends into the Ga- rich side (figure 1.4). The E_0 energies decrease with increasing [Ga]/[Cu] ratio up to 1.16. Further increase of the Ga content weakly influences the E_0 energies. This is consistent with the constancy of the lattice parameters in the compositional range from 1.16 to 1.3 reported by M. Klenk [66] .

4.2 Microstructural analysis

It is worthy to recall one of the main conclusions of the previous chapter, namely there were no second phases such as $Cu_{2-x}Se$ and/or Ga_2Se_3 detected by means of XRD within the $CuGaSe_2$ bulk and by means of GI- XRD on the film surface. For the purpose of the following section, transmission electron microscopy (TEM), in combination with energy dispersive X-ray analysis (EDX) measurements were carried out on a Ga-rich $CuGaSe_2$/Mo film with a [Ga]/[Cu] ratio of 1.14 (table 3.1). This composition corresponds to the highest efficiency ZnO/CdS/$CuGaSe_2$ solar cell devices ever prepared by the CCSVT process [44]. Figure 4.3 (a) shows an overview of the $CuGaSe_2$/Mo cross-section. $CuGaSe_2$ films consist of large grains, but relatively small ones with a submicron size are also observed in figure 4.3 (b). However, their structure is not dependant on the grain size and corresponds to that of tetragonal chalcopyrite structure. Indications of the crystallite perfection are available from the two-dimensional fast Fourier transformation (FFT) images, e.g. in the inset to figure 4.3 (b). In the $CuGaSe_2$ grains, the spacing between the (112), (200), and (220) planes are found to be of 3.2 Å, 2.8 Å, and 2.0 Å, correspondingly, in good agreement with the JCPDS-35-1100 data. The grain boundaries show highly defective regions without additional phases (figure 4.3 (b)).

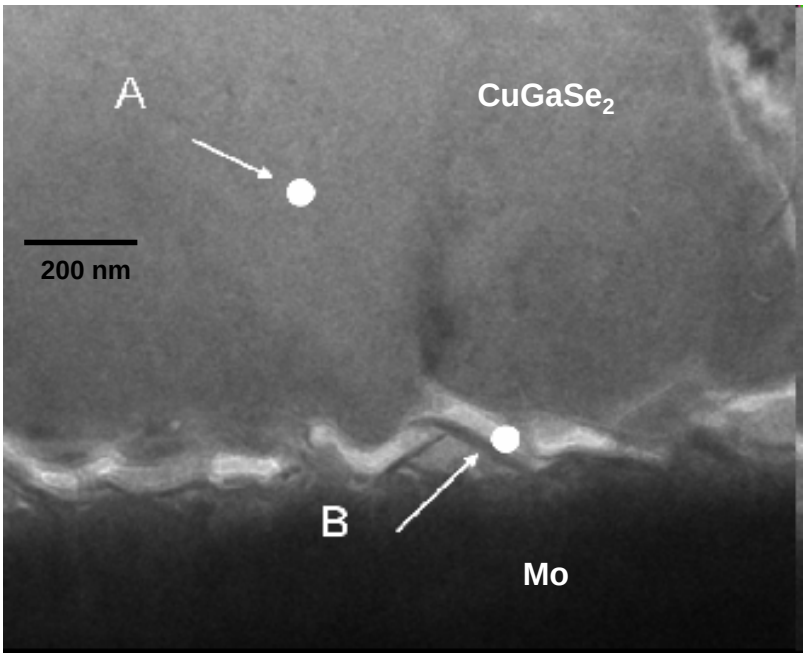

(a)

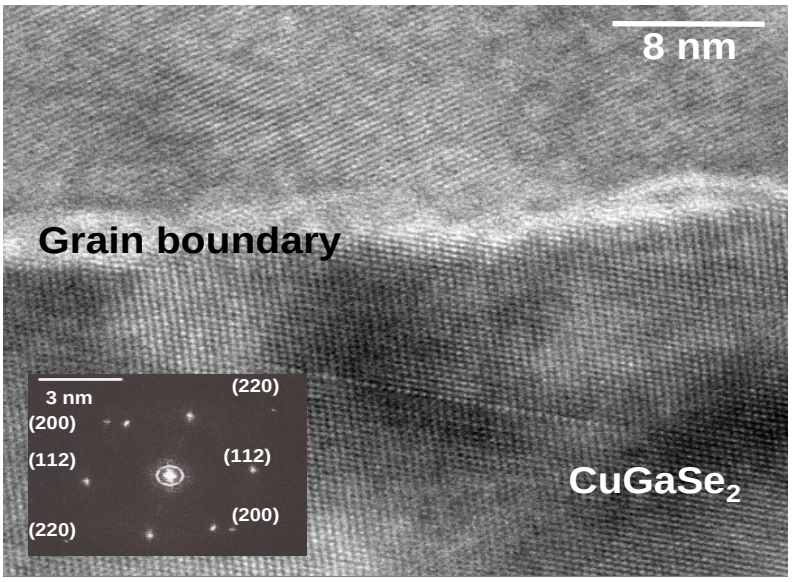

(b)

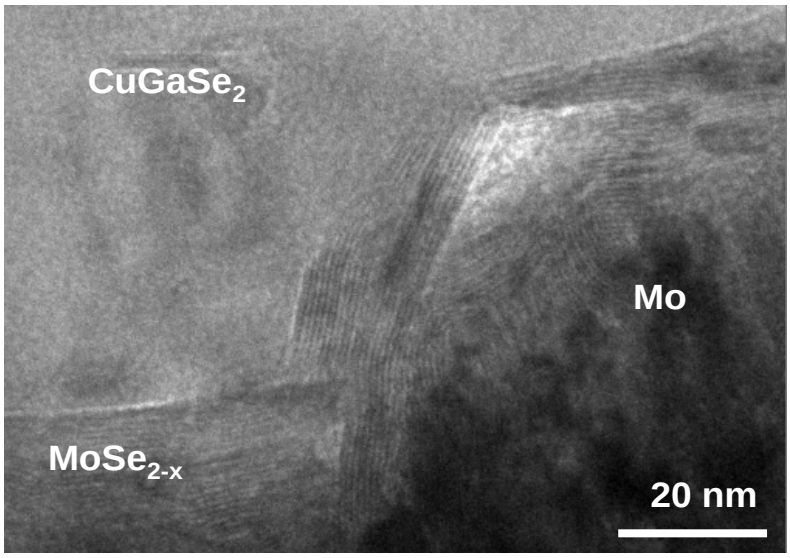

(c)

Figure 4.3. *(a) TEM cross-section of a $CuGaSe_2$/Mo/SLG structure having a composition of [Ga]/[Cu]=1.14 (table 3.1). Labels identify different layers of the heterostructure. (b) TEM micrograph of the polycrystalline $CuGaSe_2$ (region A of the figure 4.3 (a)) film involving a grain boundary between two crystallites. The inset shows a selected-area electron diffraction pattern of a $CuGaSe_2$ crystallite, proving its high crystalline quality. (c) Enlarged TEM micrograph of the $CuGaSe_2$/Mo interface at point B of the Figure 4.3 (a).*

Figure 4.3 (c) shows the TEM micrograph of the interface of $CuGaSe_2$ with Mo. The TEM pictures reveal the presence of a $\sim$ 20 – 40 nm thick interfacial layer at the rear interface between $CuGaSe_2$ and Mo. The spacing between layers corresponds to the distance between the (100) planes of the hexagonal unit cell of $MoSe_2$ according to JCPDS-20-757 data. The

presence of a $\sim$ 150 nm thick interface layer at the $CuGaSe_2$/Mo interface has been reported in [67]. It should be mentioned that the $MoSe_2$ layers in $CuGaSe_2$/Mo/SLG structure are oriented parallel to the Mo surface.

Figure 4.4 displays the energy dispersive X-ray analysis (EDX) measurements within TEM micrographs at the $CuGaSe_2$/Mo interface (area A and B of the figure 4.3 (a)). It reveals a Mo- and Se- rich composition confirming the TEM observations of the $MoSe_2$ and shows slightly different compositions for different grains. For the $CuGaSe_2$ films under consideration, [Ga]/[Cu] ratios between 1.12 $\pm$ 0.01 and 1.16 $\pm$ 0.01 were observed according to the positions A and B in the figure 4.3 (a). These values agree well with a mean value of 1.14 determined from the XRF measurements.

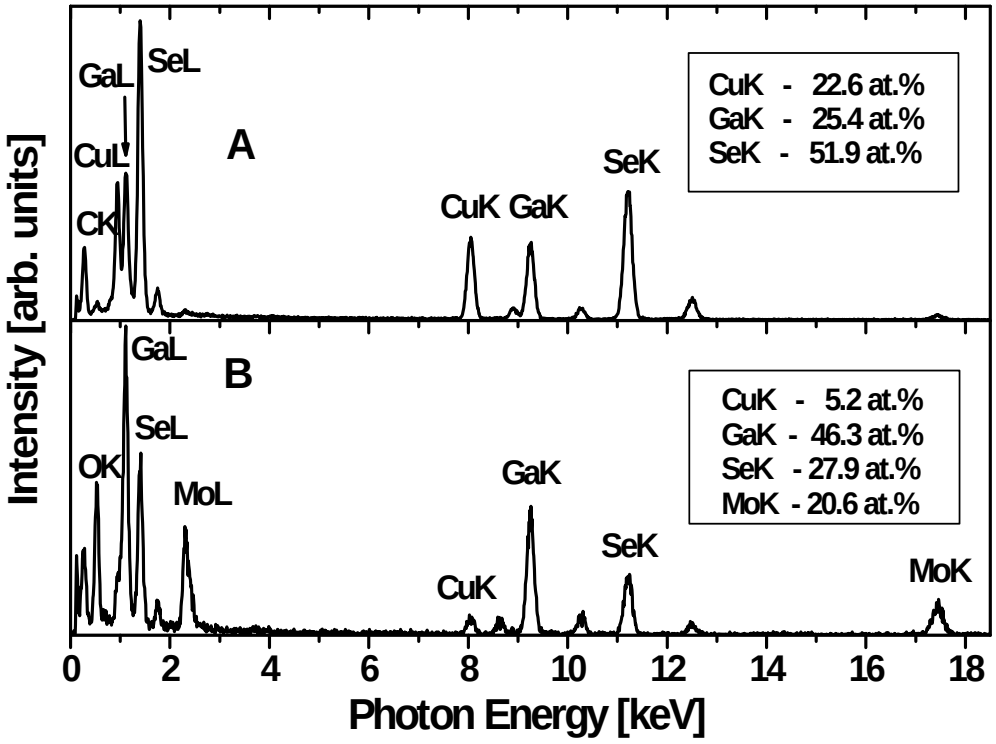

Figure 4.4. *EDX spectrum of the point (A) representative of the region in the middle of the $CuGaSe_2$ thin film and the point (B) at the $CuGaSe_2$/Mo interface. The points A and B are correspond to regions A and B in Figure 4.3 (a), respectively. The insets show the calculated concentrations of the corresponding elements.*

From the EDX spectra at the $CuGaSe_2$/Mo interface (Figure 4.4 (a), point A) a significantly higher Ga signal is recorded compared to that seen in the $CuGaSe_2$ bulk (Figure 4.4 (a), point B), while the Cu signal is reduced close to the background level. Although the spot size

of the electron beam is about 9 nm, the lateral extension of the fluorescent region within the material is larger, leading to a resolution of the point measurement of about 50 nm, which is larger than the $MoSe_2$ thickness of $\sim 20 - 40$ nm. We believe that the above mentioned Ga are located in the bright regions seen in figure 4.3 (a) between the $CuGaSe_2$ and Mo layers.

4.3 Elemental depth profiles in $CuGaSe_2$ thin films

In this section we aim at identifying the elemental composition within the depth of CCSVT grown $CuGaSe_2$ films. The depth profiling of elemental concentrations from an overall Ga-rich grown $CuGaSe_2$ film with a [Ga]/[Cu] ratio in the range 1.06 - 1.26 was extracted by means of the elastic recoil detection analysis (ERDA) technique. Relative amounts of elements as a function of the distance from the film surface are plotted in figure 4.5 for two $CuGaSe_2$ films of [Ga]/[Cu] ratio 1.11 and 1.26 as described in table 3.1. An important parameter to be taken into account during ERDA measurements is the roughness of the $CuGaSe_2$ polycrystalline film surface which will hamper both the uniform signal collection and also the homogeneous and slow removal of material by sputtering.

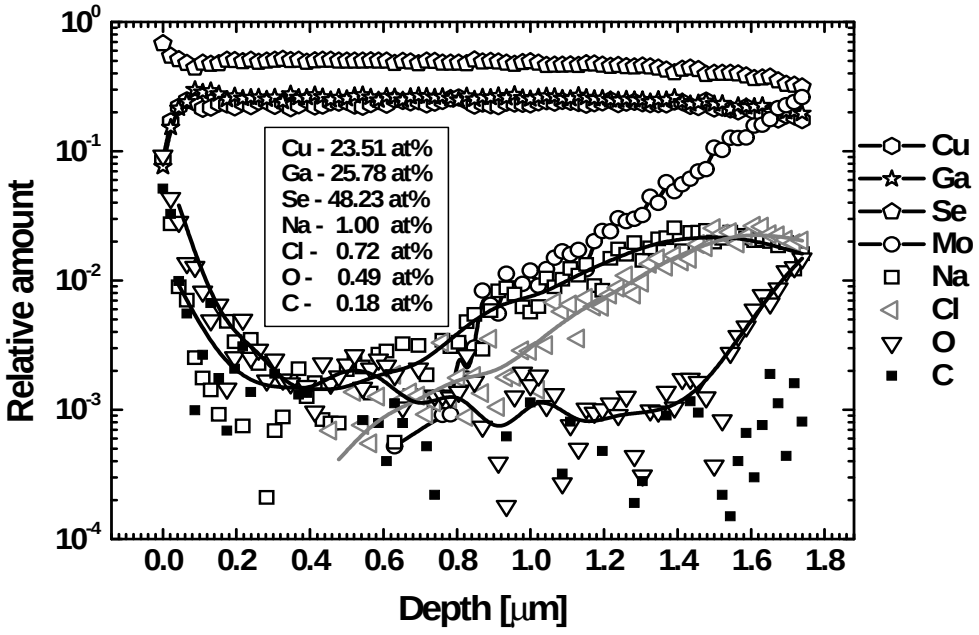

(a)

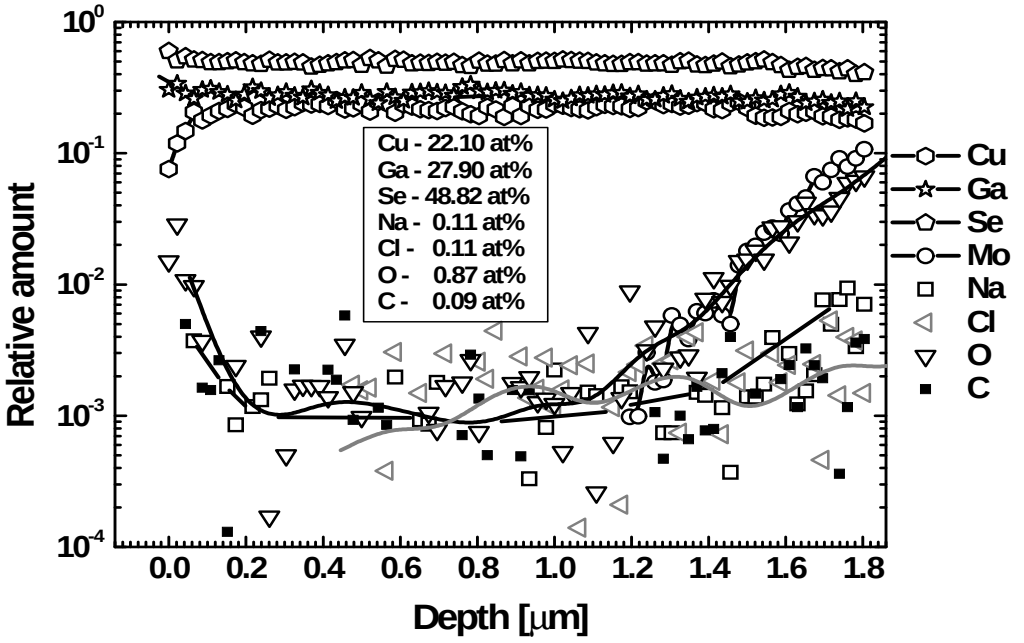

(b)

Fig 4.5 : *ERDA depth profile of elemental concentrations of the $CuGaSe_2$ thin films on Mo/SLG substrates with the ratios of (a) [Ga]/[Cu] = 1.11 and (b) [Ga]/[Cu] = 1.26 (table 3.1). The lines depict guides to the eye. The averaged elemental concentrations are inserted in the inset.*

Figures 4.5 (a) and (b) show the relative amount of the elements in dependence of the distance from the film top surface. The integral concentration of the elements Cu, Ga, and Se are nearly constant throughout the films. Meanwhile the composition of the $CuGaSe_2$ top surface changes as a function of the integral [Ga]/[Cu] ratio of the film. With increasing [Ga]/[Cu] ratio from 1.11 to 1.26, the $CuGaSe_2$ surface composition changes from Ga, Cu-poor and Se- rich (figure 4.5 (a)) to Cu- poor, and Ga, Se- rich (figure 4.5 (b)). It should be mentioned that in the compositional range investigated the film surface is always Cu poor. It is well known for this case that Cu- deficient compositions lead to the formation of $CuGa_3Se_5$ compounds on the Ga- rich film surface [64]. The composition of the front side of the film with a [Ga]/[Cu] = 1.26 is Cu:Ga:Se = 8:33:56 (figure 4.5 (b)), which corresponds approximately to the $CuGa_3Se_5$ composition. Interestingly, not only Cu, Ga, and Se were detected, but also additional elements stemming from either contaminants during the growth or from the soda lime glass substrate. Therefore, carbon and oxygen were detected at a concentration in the range 0.09 at.% - 0.18 at.% and 0.49 at.% - 0.87 at.%, respectively. Moreover, insignificant amounts of H (< 0.05 at.%) was found in all samples investigated. A higher oxygen concentration is observed closer to the $CuGaSe_2$/Mo interface in both ERDA

(figure 4.5) and EDX (figure 4.4) images. This is suggestive of oxygen diffusion from the substrate. A higher amount of Na is also found closer to the SLG substrate and the Na concentration gradually decreases in the bulk. On the film surface, Na is found with a concentration of 1 at.%. A correlation between oxygen and sodium profiles is observed: The higher the oxygen content at the $CuGaSe_2$ back side, the lower the sodium concentration at the same Mo thickness. This can be an indication that the Na transport through the Mo/SLG interface is controlled by the molybdenum oxide and not by the Mo layer itself. Similar conclusions were reached by Shklovskii [39]. The Cl concentration decreases gradually with increasing distance from the rear side and becomes undetectable at a distance of ~ 400 nm from the surface. Indeed, Cl is incorporated in the $CuGaSe_2$ during the first growth stage when the deposition occurs at high HCl concentration ($Q_{HCl}/Q_{H_2} = 10/1$) as was summarized in the figure 3.2. In the second growth stage, the Cl concentration is five times lower than that in the first one, resulting in Cl incorporation below the ERDA detection limit. Such a Cl concentration behavior correlates well with the CCSVT process stages, i.e. the growth stages and annealing.

4.4 Concluding Remarks

Microstructural and optical properties of CCSVT grown $CuGaSe_2$ thin films with various compositions have been studied by means of TEM, EDX within the TEM and ERDA, and transmission and reflectance. The results are summarized below:

- $CuGaSe_2$ thin films possess high crystalline bulk quality. Cu, Ga and Se are homogeneously distributed within the $CuGaSe_2$ bulk. The $CuGaSe_2$ surface composition is dependent on the integral [Ga]/[Cu] ratio in the film. Ga- and Cu-poor, and Se-rich surfaces are observed for nearly stoichiometric samples, whereas with increasing [Ga]/[Cu] ratio, the film top surface becomes Cu-poor, and Ga- and Se-rich, corresponding to the composition of a $CuGa_3Se_5$ compound.
- At the $CuGaSe_2$/Mo interface, a $MoSe_2$ interfacial layer is formed with a thickness ~ 20 - 40 nm. A Ga accumulation in the region of the $CuGaSe_2$/Mo interface is also observed. Na transport through the Mo/SLG interface into $CuGaSe_2$ film is limited by molybdenum oxides.
- Not only Cu, Ga, Se were found in the composition of the CCSVT prepared $CuGaSe_2$ thin films, but also elements such as carbon, oxygen originating from contamination; Na stemming from SLG and Cl introduced during the first growth stage.
- Absorption coefficient measurements have revealed three optical transitions at 1.67 eV, 1.75 eV, and 1.93 eV. With increasing [Ga]/[Cu] ratio, a "red shift" as well as a broadening of these three absorption edges was observed. The observed broadening is explained by the effect of shrinking of the $CuGaSe_2$ crystalline unit cell with increasing Ga content.